# Velocity-dependent model for the $\alpha$-$\alpha$ interaction in the context of the double-folding potential

L. C. Chamon and L. R. Gasques

*Universidade de Sao Paulo, Instituto de Fisica, Rua do Matao 1371, 05508-090 Sao Paulo, Sao Paulo, Brazil*

B. V. Carlson

*Departamento de Física, Instituto Tecnológico de Aeronáutica, Centro Técnico Aeroespacial,*
*São José dos Campos, 12228-900 Sao Paulo, Brazil*

We propose a new model to describe the $\alpha + \alpha$ interaction that takes into account the Pauli nonlocality through a velocity-dependent term. With this interaction, we describe very well the phase shifts obtained from elastic scattering data analyses for $\alpha + \alpha$ at low energies. We also obtain a good description of the *s*-wave resonance related to the $^8$Be ground-state. The model is based on double-folding procedures and, therefore, it can easily be extended to other systems. We present a test of the model in the case of elastic scattering for $^4$He $+$ $^{208}$Pb.

## I. INTRODUCTION

Heavy-ion reactions are an important subject that has been extensively studied from an experimental point of view by measuring cross sections for several processes, such as elastic and inelastic scattering, transfer reactions, breakup, and fusion. Within a theoretical context, a heavy-ion nuclear reaction is a quite complicated problem, due to the large number of nucleons involved in the collision. Some simplification is thus necessary to obtain a solution to the problem. In particular, elastic scattering data have been analyzed many times assuming the optical model (OM) approach, through the usual single-channel Schrödinger equation with a complex optical potential (OP). In this case, the corresponding imaginary part simulates the absorption of flux from the elastic channel to the reaction processes.

OM data analyses of many systems have resulted in extracted OP strengths that present significant energy dependence (see, e.g., [1]). At energies around the Coulomb barrier, the energy dependence is associated with the closure of reaction channels and is known as the threshold anomaly. In a much wider energy range, the observed energy dependence has been associated with the effective nucleon-nucleon interaction. Many theoretical models were developed to describe the energy dependence of the nuclear interaction. Among these models, the São Paulo potential (SPP) [2–5] involves a dependence of the real part of the OP on the relative velocity between the colliding nuclei. The SPP is based on double-folding procedures and also involves a systematic of nuclear densities [4]. The SPP can be used in combination with a phenomenological imaginary part of the OP that is proportional to the real one. The factor of proportionality is given approximately by $N_I \approx 0.8$ [6]. In this context, the SPP has no adjustable parameters and, thus, it is appropriate for making predictions. In this sense, the model has been extensively used in several papers as a standard OP to analyze

nuclear reactions data in a wide energy range (to date, Ref. [4] has about 500 citations).

$^4$He is a tightly bound, spherical nucleus, with its first excited state at a very high excitation energy (about 20 MeV). Therefore, it is considered to be a rather nonreactive nucleus. At energies below 34.6 MeV, the $\alpha + \alpha$ system has only one open reaction channel, the $^4$He($^4$He, $\gamma$) $^8$Be capture process, which presents a very small cross section [7–10]. Due to the lack of reaction channels, the $\alpha + \alpha$ OM elastic scattering data analyses at these energies must be performed without an imaginary part in the OP. Alternatively, the data set can also be described by adjusting phase shifts. The phase shifts should be real (no absorption), should correspond to only even angular momenta $L$ (since we deal with identical particles), and should involve just a few $L$ values, because of the low energies. In these conditions, the values of phase shifts extracted from analyses of experimental elastic scattering angular distributions have been obtained with quite good accuracy (see, e.g., [11–16]). These characteristics make the $\alpha + \alpha$ scattering at low energies a much simpler problem in comparison with heavy-ion collisions.

In an earlier paper [17], we analyzed the $\alpha + \alpha$ phase shifts at low energies in the context of the SPP. We found that, to account for the data, the strength of the SPP should be increased by about 10%. However, the renormalization factor presented some angular momentum dependence, varying from 1.081 for $L = 0$ to 1.133 for $L = 4$. In another paper [18], we analyzed the $\alpha + \alpha$ phase shifts once again, but this time with two different purposes: (i) to estimate the effects of relativity on the scattering, and (ii) to obtain a new model for the effective nucleon-nucleon interaction, with a potential based on double-folding procedures that provides a good description of the $\alpha + \alpha$ phase shifts. When dealing with energies in the range $E_{\text{lab}} < 30$ MeV, which corresponds to $v/c \leqslant 0.13$, the effect of relativity on the strength of the potential is small (about 1%). On the other hand, the nuclear

interaction obtained in that work describes very well the set of experimental phase shifts. This effective interaction, that we name here as the $\alpha$ potential, is energy independent and has a shape with a finite range of about 1.2 fm [18]. It is, therefore, quite different from the SPP, which is velocity dependent and of zero-range type [4].

Since the $\alpha$ potential is based on the double-folding approach, it is easily extended to other systems, through the corresponding nuclear densities. This potential was already applied in data analyses of several $\alpha$-nucleus systems [19,20]. The model was successful in accounting for experimental cross sections of elastic scattering, inelastic excitation, and fusion at near barrier energies, but some discrepancies were observed in the case of the elastic scattering in the backward angular region. These discrepancies could be associated with the effects of coupling to inelastic states with high excitation energies [20]. These effects were investigated assuming a schematic set of couplings in the case of the elastic scattering for $\alpha + {}^{208}$Pb, from sub-Coulomb to intermediate energies [21], assuming the energy-independent $\alpha$ potential. The conclusion of that work is that part of the observed energy dependence of the phenomenological OP that fits elastic scattering data within the OM could, in fact, be related to inelastic couplings. Indeed, the couplings assumed in [21] provide a good description of the elastic scattering data in a wide energy range of $20 \leqslant E_{\text{lab}} \leqslant 104$ MeV, but fail at higher energies ($139 \leqslant E_{\text{lab}} \leqslant 340$ MeV). Therefore, there is still room to consider significant energy dependence of the effective nucleon-nucleon interaction.

The purpose of the present paper is to include the dependence on the velocity assumed in the SPP in the $\alpha$ potential. To reach this goal, we readjust the parameters of the $\alpha$ potential by fitting the experimental $\alpha + \alpha$ phase shifts at low energies, but this time including a velocity-dependent term in the interaction. Again the $\alpha + \alpha$ potential is obtained within the context of the double-folding approach, to facilitate the extension of the model to other systems.

In the next section we provide a brief review of the SPP and $\alpha$ potential. The phase-shift analysis is presented in Sec. III. In Sec. IV, we test the new interaction in the case of the elastic scattering for ${}^{4}$He + ${}^{208}$Pb. Section V contains the main conclusions.

## II. SPP AND $\alpha$-POTENTIAL

Within the double-folding approach, the nuclear potential is obtained through

$$V(R) = \int \rho_1(\vec{r}_1)\rho_2(\vec{r}_2)u(\vec{R} - \vec{r}_1 + \vec{r}_2)\,d\vec{r}_1\,d\vec{r}_2, \quad (1)$$

where the $\rho_i$ represent the nuclear distributions and $u(\vec{r})$ is the effective interaction. In most models, $\rho_i$ is associated with the nucleon distribution of the nucleus while $u(\vec{r})$ represents the nucleon-nucleon interaction. This is not the case for the SPP and $\alpha$ potential, for which $\rho_i$ represents the matter density of the nucleus and $u(\vec{r})$ is associated to the interaction between two elementary amounts of nuclear matter [4]. The relation between matter density and nucleon distribution is analogous to the relation of charge density to the proton

TABLE I. The table presents the parameter values, volume integrals, and RMS radii related to the trial functions of equation (3), obtained in [18]. The units assumed for these values are $U_0$ (MeV), $a$ and $r_{\text{RMS}}$ (fm), $V_0$ (MeV fm$^3$).

| Label | $f(r)$ | $U_0$ | $a$ | $V_0$ | $r_{\text{RMS}}$ |
|---|---|---|---|---|---|
| 1 | $e^{-(r/a)^2}$ | 87.226 | 0.95 | 416.4 | 1.164 |
| 2 | $e^{-r/a}$ | 330.61 | 0.37 | 420.9 | 1.282 |
| 3 | $r\,e^{-(r/a)^2}$ | 161.22 | 0.80 | 414.9 | 1.131 |
| 4 | $r\,e^{-r/a}$ | 1042.0 | 0.27 | 417.5 | 1.207 |

distribution. In the case of the $\alpha$ particle, the corresponding matter density is equal to the respective charge density multiplied by 2 (due to the normalization of the densities). We assume that the ${}^4$He charge density is obtained from electron scattering experiments [22].

The effective nuclear interaction of the SPP is given by [4]

$$u(\vec{r}) = -V_0\,\delta(\vec{r})\,e^{-4v_{\text{REL}}^2/c^2}, \quad (2)$$

where $V_0 = 456$ MeV fm$^3$, $c$ is the speed of light, and $v_{\text{REL}}$ represents the local relative velocity between the two nuclei. This dependence on the velocity is associated to the Pauli nonlocality that arises from the exchange of nucleons between target and projectile [2–4]. Due to the $\delta$ function involved in this equation, the SPP effective nuclear interaction is obtained within a zero-range approach. An alternative finite range effective nucleon-nucleon interaction can also be obtained for the SPP within this context [4].

In the case of the $\alpha$-potential, $\rho_i$ still represents the matter density of the nucleus. In [18], we assumed the following model for the effective nuclear interaction:

$$u(\vec{r}) = -U_0\,f(r), \quad (3)$$

where the function $f(r)$ involves one adjustable parameter. Four trial shapes for $f(r)$ were tested in the fits to the $\alpha + \alpha$ phase-shift data. The adjustments were not sensitive to the shape assumed for $f(r)$. Probably this behavior is related to the fact that the four trial functions resulted in quite similar values for the corresponding volume integral ($V_0$) and root-mean square radius ($r_{\text{RMS}}$):

$$V_0 = U_0\,4\pi \int_0^\infty f(r)\,r^2\,dr, \quad (4)$$

$$r_{\text{RMS}} = \sqrt{\frac{\int_0^\infty f(r)\,r^4\,dr}{\int_0^\infty f(r)\,r^2\,dr}}. \quad (5)$$

The parameter values, volume integrals, and RMS radii of these $f(r)$ functions, obtained in [18], are provided in Table I.

## III. PHASE-SHIFTS ANALYSIS

From now on, we assume the following model for the effective nuclear interaction:

$$u(\vec{r}) = -U_0\,f(r)\,e^{-4v_{\text{REL}}^2/c^2}. \quad (6)$$

TABLE II. The same as Table I, but now considering Eq. (6) for the intrinsic nuclear interaction.

| Label | $f(r)$ | $U_0$ | $a$ | $V_0$ | $r_{RMS}$ |
|---|---|---|---|---|---|
| 1 | $e^{-(r/a)^2}$ | 735.813 | 0.50 | 512.2 | 0.612 |
| 2 | $e^{-r/a}$ | 4139.55 | 0.17 | 511.1 | 0.589 |
| 3 | $r\,e^{-(r/a)^2}$ | 2617.10 | 0.42 | 511.7 | 0.594 |
| 4 | $r\,e^{-r/a}$ | 20432.8 | 0.135 | 511.7 | 0.604 |

Although here we analyze only data at low energies, we relate the local relative velocity to the kinetic energy in terms of the theory of relativity:

$$E_K(R) = E - V_C(R) - V_N(R), \tag{7}$$

$$v^2(R)/c^2 = 1 - \left(\frac{\mu c^2}{\mu c^2 + E_K(R)}\right)^2. \tag{8}$$

$V_C$ is the Coulomb potential (which is also calculated through a folding procedure) and $\mu$ is the reduced rest mass of the system. The nuclear interaction between the $\alpha$ particles, $V_N(R)$, is calculated according to (1) and (6) and is assumed to be the real part of the OP in the $\alpha + \alpha$ phase-shift analysis. As already commented, no imaginary part is included in the OP.

For $f(r)$, we adopt the same trial functions used in [18]. These functions involve two parameters, $U_0$ and $a$, for which the corresponding values were obtained from the phase-shift fits. The best fit parameter values are presented in Table II, which also includes the corresponding volume integrals and RMS radii.

Figure 1 presents the $\alpha + \alpha$ experimental phase shifts from [11–16] for $L = 0$, 2, and 4. We used the fact that the phase shifts can be changed by multiples of 180 degrees to avoid overlapping values for different angular momenta. All four trial functions of Table II provide quite similar and very good data fits, represented by the solid lines in Fig. 1.
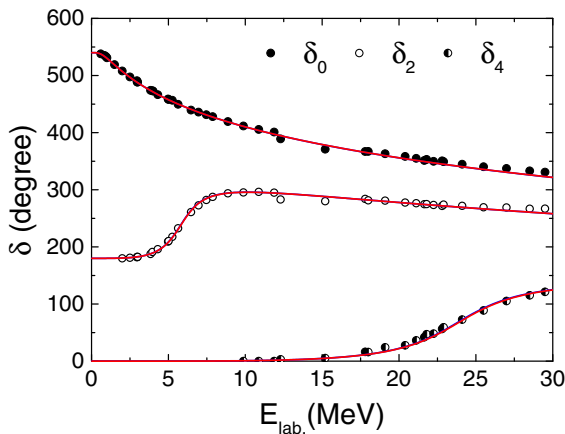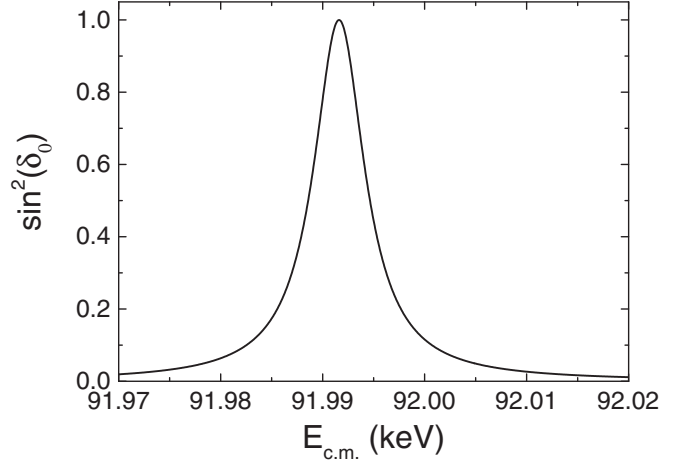


FIG. 2. $\sin^2(\delta_0)$ obtained with our theoretical calculations as a function of the $\alpha + \alpha$ center-of-mass energy.

The $U_0$ values of Table II are presented with six digits, which represents a precision much higher than that obtained through the phase-shift fits. In fact, this precision was obtained from the fit of the known $s$-wave resonance of the $^8$Be ground state. $^8$Be is unbound, with an experimental $Q$ value (relative to the two-$\alpha$ channel) of about 92 keV and a width of about 6 eV. Figure 2 shows the behavior of $\sin^2(\delta_0)$ as a function of the energy of the $\alpha + \alpha$ system (in the center-of-mass frame), obtained with our theoretical calculations.

As already mentioned, the four functions of Table II provide almost identical fits of the $\alpha + \alpha$ phase shifts. On the other hand, these functions have quite different shapes, as illustrated in Fig. 3(a). Even so, due to the double-folding procedure involved in Eq. (1), the resulting nuclear potentials (obtained assuming these four functions) are very similar for most of the systems. In order to illustrated this point, we have calculated the nuclear potentials for three different systems: proton-proton, proton-$\alpha$, and $\alpha$-$\alpha$, which are presented in



FIG. 1. Comparison between experimental phase shifts for $L = 0$, 2, and 4 and the theoretical results obtained with trial function 1 of Table II.
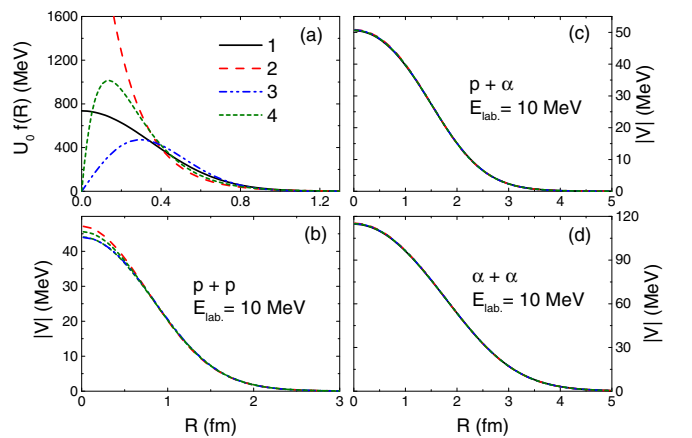


FIG. 3. (a) $U_0 f(r)$ as a function of $r$. The labels of these functions are the same as indicated in Table II. The figure also presents the nuclear potential obtained with the four trial functions, for the (b) proton-proton, (c) proton-$\alpha$, and (d) $\alpha$-$\alpha$ systems.
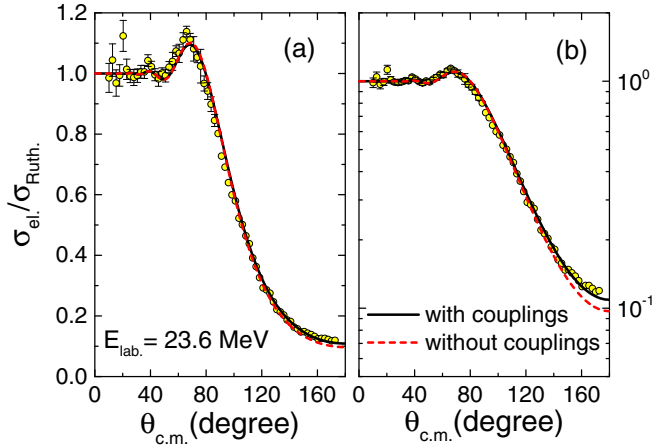
FIG. 4. Experimental and theoretical elastic scattering angular distributions for $^4$He + $^{208}$Pb at $E_{lab.} = 23.6$ MeV. Note the change from (a) linear to (b) logarithmic scale. The solid black and dotted red lines correspond to calculations performed with and without the couplings to the inelastic states, respectively.

Figs. 3(b), 3(c) and 3(d). Only for the proton-proton system is it possible to see (at internal distances) small differences among the nuclear potentials obtained with different $U_0 f(r)$. For proton-$\alpha$ and $\alpha$-$\alpha$ the nuclear potentials obtained with the four functions of Table II are almost indistinguishable. We have verified that even smaller differences are obtained for heavier systems.

## IV. TEST OF THE MODEL

Since the nuclear potential is obtained from the double-folding method, the $\alpha$ potential can be extended to other systems. In order to test the model, we have chosen, as example, the $^4$He + $^{208}$Pb system. We selected two experimental elastic scattering angular distributions to perform our analyses: one at $E_{lab.} = 23.6$ MeV, which is slightly above the Coulomb barrier, and the other at $E_{lab.} = 139$ MeV (about 35 MeV/nucleon) from [23,24].

The present model of the $\alpha$ potential with the velocity-dependent term was adopted for the real part of the OP in our theoretical calculations. In the case of $E_{lab.} = 23.6$ MeV, we adopted a Woods-Saxon potential for the imaginary part of the OP, with parameter values of $R_I = 6$ fm, $a_I = 0.25$ fm, and $W_0 = 60$ MeV. The same imaginary potential was used in [20], where the $\alpha$ potential without the velocity-dependent term was assumed for the real part of the OP. These values result only on internal absorption, in order to simulate the fusion process. We have also considered the inelastic couplings to the first $2^+$ and $3^-$ $^{208}$Pb excited states, with the same deformation parameters of [20].

Figure 4 shows data and theoretical elastic scattering angular distributions for $E_{lab.} = 23.6$ MeV, using (a) linear and (b) logarithmic scales. The solid black and dotted red lines in the figure correspond to calculations performed with or without the couplings to the inelastic states, respectively. The effect of the couplings is quite small at this low energy and the theoretical results are in quite good agreement with the data.
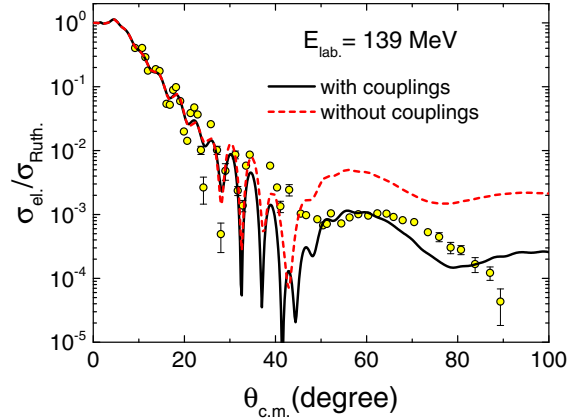


FIG. 5. Experimental and theoretical elastic scattering angular distributions at $E_{lab.} = 139$ MeV. The solid black and dotted red lines correspond to calculations performed with and without the coupling to the inelastic states.

In the case of $E_{lab.} = 139$ MeV, the use of an internal imaginary potential is not adequate since significant peripheral reactions should occur at high energies. Thus, we still assumed a Woods-Saxon shape for the imaginary part of the OP, but in this case we adjusted the corresponding parameters through a fit to data. We obtained $R_I = 9.9$ fm, $a_I = 0.812$ fm, and $W_0 = 12$ MeV. Data and theoretical results for this energy are shown in Fig. 5. The theoretical cross sections agree well with the data in the forward angular region, but the fit is not satisfactory for backward angles. Note that the effect of the inelastic couplings on the elastic channel is quite significant only in the backward region. Thus, as already discussed in [21], where, in order to obtain a better fit to the data at this high energy, it is necessary to consider many other couplings. This goal is beyond the scope of the present work.

## V. CONCLUSION

In the present paper, we have included the velocity dependence of the SPP model in the context of the $\alpha$-potential approach. With this theoretical model, we obtain a quite good adjustment of the experimental $\alpha + \alpha$ phase shifts, as well as a description of the $s$-wave resonance of the $^8$Be ground state. These results do not depend on the shape assumed for the four trial functions adopted in our calculations. On the other hand, all of the functions provided similar volume integrals and RMS radii: $V_0 \approx 512$ MeV fm$^3$ and $r_{RMS} \approx 0.60$ fm (see Table II). These values should be compared with those from the SPP [see Eq. (2)]: $V_0 = 456$ MeV fm$^3$ and $r_{RMS} = 0$ (zero-range approach). In fact, an increase of about 10% in the SPP strength is necessary to describe the $\alpha + \alpha$ phase shifts, as reported in an earlier work [17]. This behavior is compatible with the volume integral difference found here for the $\alpha$ potential in comparison with the SPP. An important inconvenience of the SPP in accounting for the $\alpha + \alpha$ phase shifts is the (slight) angular momentum dependence of the renormalization factor necessary to fit the data. This problem does not exist within the $\alpha$-potential approach, because of the additional degree of freedom involved in the respective

adjustment of the interaction range. In fact, as already commented, the $\alpha$ potential has $r_{\mathrm{RMS}} \approx 0.60$ fm while the SPP is of zero range. The present effective nuclear interaction of the $\alpha$ potential can thus be considered as an improvement of the SPP.

Since the $\alpha$ potential is obtained through a double-folding procedure, the model can easily be extended to other systems. In particular, the model should be useful to investigate the effect of the dependence on the velocity for $\alpha$-nucleus systems at high energies. We provided a test of the model through elastic scattering data analyses for $^4\mathrm{He} + {}^{208}\mathrm{Pb}$. For $E_{\mathrm{lab.}} = 23.6$ MeV, near the Coulomb barrier, our theoretical model provided an excellent description of the data set, without adjusting any parameter related to the imaginary part of the OP. For $E_{\mathrm{lab.}} = 139$ MeV, about 35 MeV/nucleon, we obtained a good data fit for forward angles but the fit to the data is not satisfactory in the backward region. In this region, the theoretical elastic scattering cross section is very sensitive to inelastic couplings. Therefore, the fit could probably be improved if many other inelastic couplings were included in the calculations, as proposed earlier in [21]. Even so, the results obtained in the present work show that the $\alpha$ potential should be useful in data analyses of $\alpha$-nucleus and heavy-ion systems at low and high energies.

[1] M. E. Brandan and G. R. Satchler, Phys. Rep. **285**, 43 (1997).

[2] M. A. Candido Ribeiro, L. C. Chamon, D. Pereira, M. S. Hussein, and D. Galetti, Phys. Rev. Lett. **78**, 3270 (1997).

[3] L. C. Chamon, D. Pereira, M. S. Hussein, M. A. Candido Ribeiro, and D. Galetti, Phys. Rev. Lett. **79**, 5218 (1997).

[4] L. C. Chamon, B. V. Carlson, L. R. Gasques, D. Pereira, C. De Conti, M. A. G. Alvarez, M. S. Hussein, M. A. Candido Ribeiro, E. S. Rossi, Jr., and C. P. Silva, Phys. Rev. C **66**, 014610 (2002).

[5] L. C. Chamon, Nucl. Phys. A **787**, 198c (2007).

[6] M. A. G. Alvarez, L. C. Chamon, M. S. Hussein, D. Pereira, L. R. Gasques, E. S. Rossi, Jr., and C. P. Silva, Nucl. Phys. A **723**, 93 (2003).

[7] K. Langanke and C. Rolfs, Z. Phys. A **324**, 307 (1986).

[8] K. Langanke and C. Rolfs, Phys. Rev. C **33**, 790 (1986).

[9] V. M. Datar, S. Kumar, D. R. Chakrabarty, V. Nanal, E. T. Mirgule, A. Mitra, and H. H. Oza, Phys. Rev. Lett. **94**, 122502 (2005).

[10] P. Mohr *et al.*, Z. Phys. A **349**, 339 (1994).

[11] J. L. Russel, Jr., G. C. Phillips, and C. W. Reich, Phys. Rev. **104**, 135 (1956).

[12] N. P. Heydenburg and G. M. Temmer, Phys. Rev. **104**, 123 (1956).

[13] R. Nilson, R. O. Kerman, G. R. Brigs, and W. K. Jentschke, Phys. Rev. **104**, 1673 (1956).

[14] R. Nilson, W. K. Jentschke, G. R. Brigs, R. O. Kerman, and J. N. Snyder, Phys. Rev. **109**, 850 (1958).

[15] T. A. Tombrello and L. S. Senhouse, Phys. Rev. **129**, 2252 (1963).

[16] W. S. Chien and Ronald E. Brown, Phys. Rev. C **10**, 1767 (1974).

[17] L. C. Chamon, B. V. Carlson, and L. R. Gasques, Phys. Rev. C **83**, 034617 (2011).

[18] L. C. Chamon, L. R. Gasques, and B. V. Carlson, Phys. Rev. C **84**, 044607 (2011).

[19] L. C. Chamon, L. R. Gasques, L. F. M. Alves, V. Guimarães, P. Descouvemont, R. J. deBoer, and M. Weischer, J. Phys. G **41**, 035101 (2014).

[20] L. C. Chamon, L. R. Gasques, G. P. A. Nobre, E. S. Rossi, Jr., R. J. deBoer, M. Weischer, and G. G. Kiss, J. Phys. G **42**, 055102 (2015).

[21] L. C. Chamon and L. R. Gasques, J. Phys. G **43**, 015107 (2016).

[22] H. De Vries, C. W. De Jager, and C. De Vries, At. Data Nucl. Data Tables **36**, 495 (1987).

[23] W. Karcz, I. Kluska, Z. Sanok, J. Szmider, J. Szymakowski, S. Wiktor, and R. Wolski, Acta Phys. Pol. B **3**, 525 (1972).

[24] D. A. Goldberg, S. M. Smith, H. G. Pugh, P. G. Roos, and N. S. Wall, Phys. Rev. C **7**, 1938 (1973).